




# Highly photoluminescent water-soluble ZnSe/ZnS/ZnS quantum dots via successive shell growth approach

Xiaoyan Li<sup>1</sup> , Hongyan Zou<sup>1</sup>, Mingzhong Wang<sup>1</sup>, Weichen Wang<sup>1</sup>, Boxu Yang<sup>1</sup>, and Xiaopeng Zhao<sup>1,\*</sup>

<sup>1</sup> Smart Materials Laboratory, Department of Applied Physics, Northwestern Polytechnical University, Xi'an 710129, People's Republic of China

**Received:** 7 November 2021

**Accepted:** 25 April 2022

**Published online:**  
14 May 2022

© The Author(s), under exclusive licence to Springer Science+Business Media, LLC, part of Springer Nature 2022

## ABSTRACT

ZnSe quantum dots (QDs) are considered to be the most promising alternative to Cd-based QD owing to their distinct optical properties and low toxicity. In this paper, we develop an efficient and simple method to prepare a water-soluble ZnSe/ZnS/ZnS core/shell/shell heterostructure QDs for the first time. In this strategy, the ZnSe core is first coated with ZnS, then the second ZnS shell is loaded on ZnSe/ZnS by growing successively. The prepared ZnSe/ZnS/ZnS QDs with the merit of environmentally friendly show a uniformly dispersed spherical structure, and the photoluminescence (PL) intensity of ZnSe/ZnS/ZnS is 3.1 and 1.3 times as large as that of ZnSe and ZnSe/ZnS. In addition, the prepared QDs have good dispersion in water and remain the stability for at least 30 days without sedimentation. The excellent performance of ZnSe/ZnS/ZnS is ascribed to the mercaptopropionic (MPA) is used as an effective stabilizer for the QDs and the second ZnS shell that effectively inhibits the exciton leakage.

## 1 Introduction

Quantum dots (QDs) are increasingly being utilized in light-emitting devices (LEDs) [1–6], photodiodes [7], solar cells [8–10], biological analysis [11–13] owing to their interesting optical properties. So far, researchers have successfully synthesized a large number of high-quality QDs [14–17]. However, most reported research is primarily focusing on Cd-based QDs; the drawbacks of which are causing serious chronic diseases and cancers and limits their applicability in the devices [18, 19].

ZnSe QDs are considered a material with great potential to replace Cd-based QDs due to their low toxicity (without heavy metal ions). Shen et al. used octadecene (ODE) as a non-coordination solvent to prepare monodisperse ZnSe QDs with sphalerite structure, and the luminescence wavelength moved from 400 to 500 and 600 nm by doping [20]. Senthilkumar et al. obtained the ZnSe QDs with high photoluminescence by wet chemical approach [21]. Zhang et al. synthesized ZnSe nanocrystals in an aqueous solution by using glutathione (GSH) as ligand, the results showed that the photoluminescence quantum yield of the ZnSe QDs will be affected

Address correspondence to E-mail: xpzhao@nwpu.edu.cn

by the pH of the system [22]. Although researchers have successfully synthesized a large number of ZnSe QDs, the small size of ZnSe QDs manifested a large surface effect, which introduced some unsaturated and dangling bonds, the luminous efficiency, and stability of single-core QDs are significantly lower than that of other types of QDs [23]. Therefore, it is of importance to improve the luminescence quality of ZnSe QDs for expanding the application in optoelectronic devices and biomedicine analysis and superconductor [24, 25]. Considerable efforts have been devoted to improving the luminous efficiency and the stability of QDs [26, 27]. One of the effective ways to improve the fluorescence efficiency and stability of ZnSe QDs is growing a ZnS shell with a wider bandgap on the ZnSe core [28]. Nikesh et al. coated ZnS monolayer on ZnSe QDs for passivating the surface states and reducing the leakage of the hole in the ZnSe core and resulting in high PL efficiency [29]. Fang et al. prepared ZnSe/ZnS in an aqueous solution to improve the stability of the ZnSe QDs [30]. Wang et al. used the thermal injection method to prepare monodisperse ZnSe/ZnS QDs, the prepared QDs have superior chemical and photochemical stability [31].

However, one non-negligible issue is that the electrons and holes in ZnSe are still diffused to the shell of ZnS or reach the surface of QD, which can interact with the surrounding environment and reduce the luminous efficiency [32]. The core/shell/shell structure of QDs helps to further limit the electrons and holes and passivate surface defects for enhancing luminous efficiency [33]. Wood et al. synthesized ZnSe/ZnS: Mn/ZnS QDs using the hot injection method, and studied the ac-driven electroluminescence from prepared QDs [34]. Yang et al. reported a seed-mediated synthesis ZnSe/ZnS/ZnS QDs with high PL efficiency at 300 °C by using trioctylphosphine (TOP) as solvent [35]. The reported method previously for the synthesis of QDs is mainly using toxic organic solvents at high temperatures, and the synthesis conditions are complicated and harmful to the environment.

Herein, we present a green and rapid route for synthesizing the environmentally friendly ZnSe/ZnS/ZnS QDs in the aqueous solution for the first time (to the best of our knowledge). The PL intensity of ZnSe/ZnS/ZnS is 3.1 and 1.3 times as large as that of ZnSe and ZnSe/ZnS. In addition, the prepared QDs have good dispersion in water and remain the

stability for at least 30 days without sedimentation. The successive growth method without purification between each growth step has the advantages of low reaction temperature, operating simple and low cost. Our method paves a new way for the industrial purposes of ZnSe QDs and also has a non-negligible environmental significance.

## 2 Experiment section

### 2.1 Chemicals

Zinc nitrate ( $\text{Zn}(\text{NO}_3)_2$ ,  $\geq 99\%$ ), zinc acetate ( $\text{Zn}(\text{OAc})_2$ ,  $\geq 99.0\%$ ), selenium powder ( $\text{Se}$ ,  $\geq 99\%$ ), sodium borohydride ( $\text{NaBH}_4$ ,  $\geq 99\%$ ), thiourea ( $\geq 99\%$ ), and sodium hydroxide ( $\text{NaOH}$ ,  $\geq 99\%$ ) were purchased from Tianjin Damao Chemical Reagent Factory. Mercaptopropionic acid (MPA, 99%) was purchased from Beijing Bailingwei Technology Co., Ltd., the above reagents were all analytically pure. The experimental water was deionized water, which was prepared by the Exceed-Cd-16 ultrapure water machine.

### 2.2 Preparation

#### 2.2.1 Preparation of precursor solution

Preparation of Zn precursor solution: MPA (6 mmol) was mixed with 5 mmol of  $\text{Zn}(\text{NO}_3)_2 \cdot 6\text{H}_2\text{O}$  solution, the pH of the mixture was adjusted to 10.30, and blow nitrogen for 30 min to remove dissolved oxygen in the solution.

Preparation of Se precursor solution: 13.50 mmol of sodium borohydride was dissolved in deionized water, then added selenium powder (4.50 mmol), the reaction vessel needs a hole to release the  $\text{H}_2$  during the reaction until the black selenium powder disappears completely, then sodium hydrogen selenide ( $\text{NaHSe}$ ) solution (0.5 mol/L) was obtained.

ZnS precursor solution:  $\text{Zn}(\text{Ac})_2 \cdot 6\text{H}_2\text{O}$  (3.75 mmol), MPA (5.63 mmol), and thiourea (3.75 mmol) were dissolved in deionized water.

#### 2.2.2 Preparation of ZnSe/ZnS/ZnS QDs

Preparation of ZnSe core according to the method was reported by Wang [36] and some modifications were made, the steps are shown in Fig. 1. In a typical

procedure, 2.50 mmol of fresh NaHSe solution was added into the Zn precursor solution. The mixture was maintained at 100 °C under N<sub>2</sub> for 4.5 h to obtain the ZnSe QDs solution. To synthesize ZnSe/ZnS/ZnS QDs, for the first step, ZnS precursor and prepared ZnSe QDs solution was mixed in a certain proportion, and the mixture was maintained at 90 °C under N<sub>2</sub> for 1.5 h, ZnSe/ZnS QDs were obtained. Then, the above operation was repeated to obtain ZnSe/ZnS/ZnS QDs. Finally, the reaction mixture was precipitated by ethanol, and the products were washed three times with ethanol and deionized water respectively, white powder sample was obtained after drying in a vacuum.

### 2.3 Characterizations

The chemical bond of the sample was characterized by FT/IR-400plus VIR-9000 Fourier spectrometer. The phase composition of the samples was characterized by a Hitachi XRD-7000 diffractometer. The morphology of the ZnSe/ZnS/ZnS was observed by an FEI Talos F200X transmission electron microscope (TEM). XPS (Axis Supra, Kratos, Japan) was performed using a monochromatized Al-Ka source. Photoluminescence (PL) properties were studied using a Hitachi F-7000 fluorescence spectrophotometer. HERMLE Z323 centrifuge and ZK82J vacuum drying box were used to purify the QDs.

## 3 Results and discussion

The X-ray diffraction (XRD) pattern of the ZnSe/ZnS/ZnS together with that of ZnSe and ZnSe/ZnS are shown in Fig. 2. From Fig. 2, it can be seen that the diffraction peaks approximately at 27.40°, 45.40°, and 53.53° are corresponding to the (111), (220), and (311) crystal planes (PDF#37-1463), respectively, which indicates that the ZnSe/ZnS/ZnS adopt a cubic sphalerite structure similar to that of ZnSe and ZnSe/ZnS and no diffraction peak of ZnS (PDF#

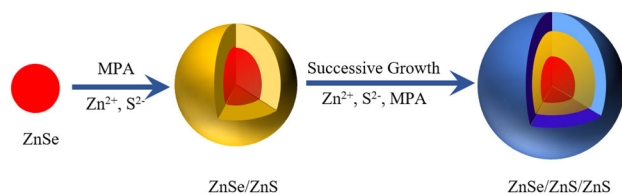


**Fig. 1** Schematic illustration of ZnSe/ZnS/ZnS QDs synthesis

05-0566) are observed in XRD analysis. It can also be proved that the ZnS is grown in the outer core of ZnSe rather than pure ZnS crystal [37]. In addition, we can see a significant broadening of diffraction peak from ZnSe/ZnS/ZnS, which is caused by the small crystallite size of ZnSe/ZnS/ZnS.

TEM was performed to characterize the morphologies of prepared quantum dots. From Fig. 3a, one can see that ZnSe/ZnS/ZnS QDs show a uniformly dispersed spherical structure without agglomeration, with an average size of about 11 nm, illustrating that the MPA is used as an effective dispersant for QDs. To explain the reason for the improved dispersion of ZnSe/ZnS/ZnS by MPA, the FT-IR patterns of prepared QDs are shown in Fig. 3b. We can see that the FT-IR spectrum of ZnSe/ZnS/ZnS is very similar to that of ZnSe and ZnSe/ZnS, exhibiting the strong bands of asymmetric and symmetric stretching of COO<sup>-</sup> at 1566 cm<sup>-1</sup> and 1403 cm<sup>-1</sup>, respectively. Meanwhile, the S–H stretching vibration band at 2524 cm<sup>-1</sup> is absent in the FTIR spectrum of the MPA-capped QDs, which indicates that the S–H bond in the MPA is destroyed by forming a Zn–S coordinate bond between MPA and QDs due to the high affinity between S and Zn [36, 38, 39]. In addition, the absence of the peak at 2524 cm<sup>-1</sup> in the MPA-capped QDs spectra is also prove that MPA has been successfully modified to the surface of QDs. The hydrophilic carboxyl group with the negative charge of the MPA molecules can separate the QDs into individual spherical particles in an aqueous solution, which was confirmed from the result in TEM.

To further characterize the synthesized QDs, we carried out XPS to investigate the surface

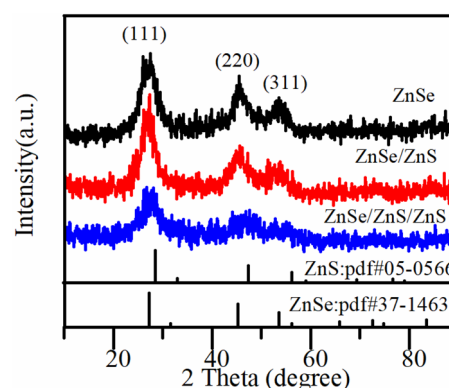
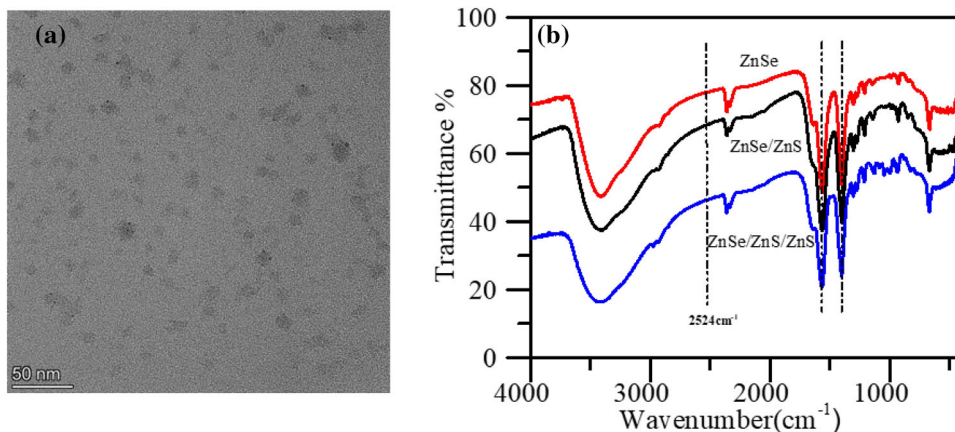


**Fig. 2** XRD patterns of ZnSe, ZnSe/ZnS and ZnSe/ZnS/ZnS, respectively

**Fig. 3** **a** TEM images of ZnSe/ZnS/ZnS. **b** FT-IR spectra of ZnSe, ZnSe/ZnS and ZnSe/ZnS/ZnS, respectively

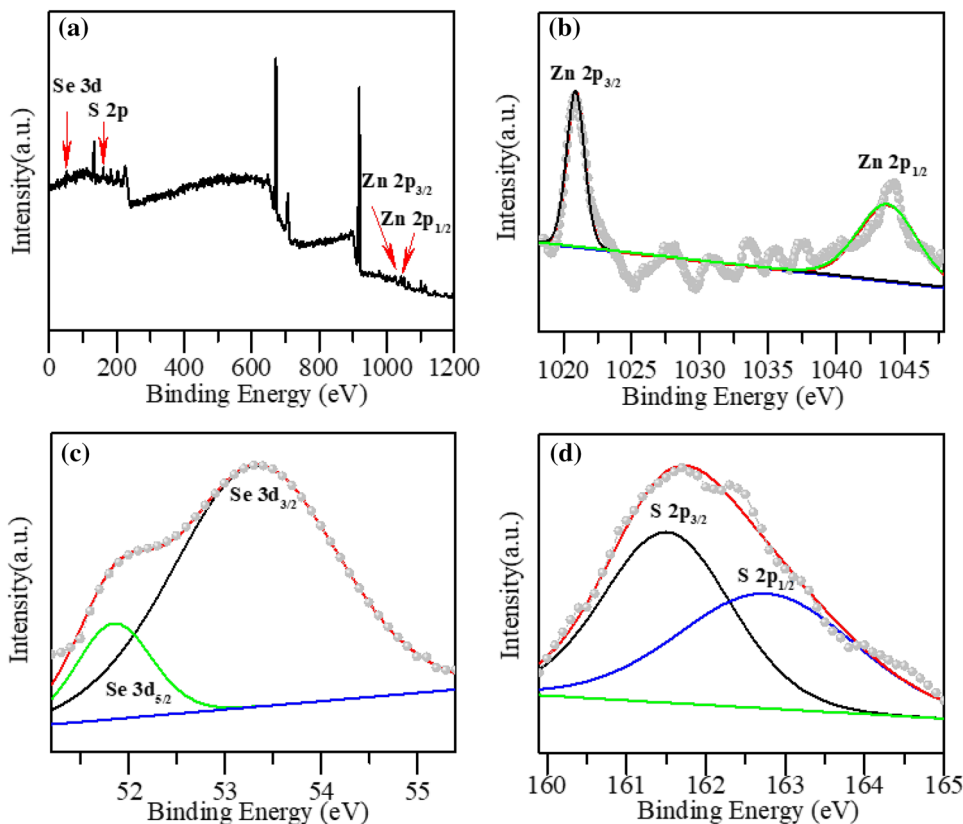


composition of ZnSe/ZnS/ZnS, and the results are shown in Fig. 4. In Fig. 4, the characteristic peaks of Zn  $2p_{3/2}$ , Zn  $2p_{1/2}$ , Se  $3d_{5/2}$ , and Se  $3d_{3/2}$  are located at 1021.01, 1043.81, 51.87, and 53.38 eV, respectively, indicating the existence of Zn<sup>2+</sup> and Se<sup>2-</sup> (Fig. 4b and c) [40], the characteristic peaks of S 2p located at 161.52 and 162.75 eV is attributed to the characteristic peak of S<sup>2-</sup> in ZnS (Fig. 4d).

Figure 5a presents PL spectra of various prepared QDs. Compared with ZnS (magenta curve), one can see that the emission peaks at 402 nm and 450 nm are

obtained on the ZnSe (red curve), ZnSe/ZnS (black curve), and ZnSe/ZnS/ZnS (blue curve), respectively, which is attributed to the band-edge and defect-related emission peak of zinc selenide. It is noticeable that the PL intensity of ZnSe/ZnS/ZnS is much higher than that of ZnSe and ZnSe/ZnS, which was 3.1 and 1.3 times as large as that of ZnSe and ZnSe/ZnS. Meanwhile, the intensity ratio of the band-edge emission to the defect-related emission is increased from 1.27 to 1.29 and 1.31 with the growth of the shell. It is shown that the PL intensity of ZnSe

**Fig. 4** XPS spectra of ZnSe/ZnS/ZnS quantum dots (a), Zn 2p (b), Se 3d (c), and S 2p (d), respectively





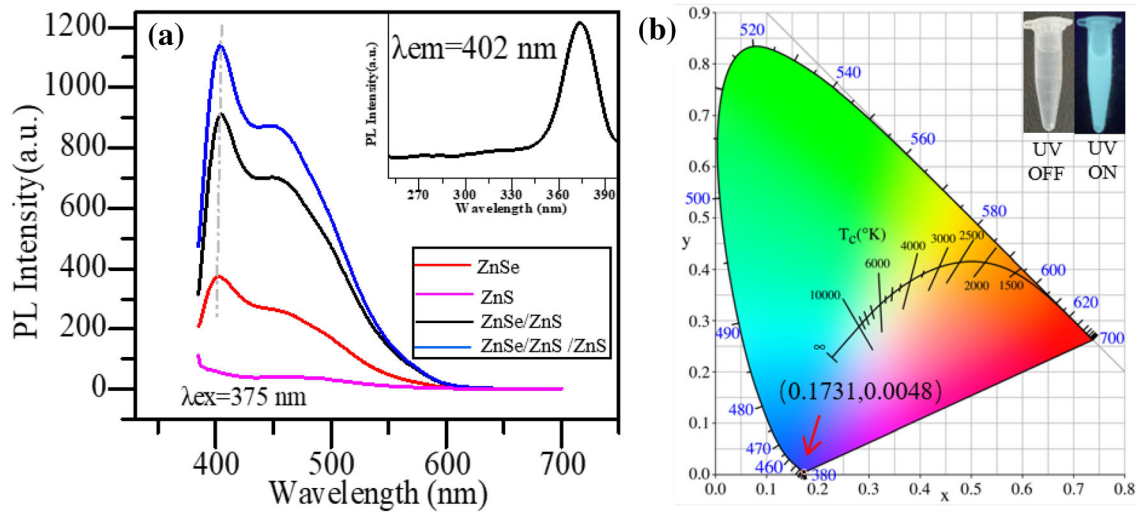


**Fig. 5** **a** Photoluminescence of ZnS, ZnSe, ZnSe/ZnS and ZnSe/ZnS/ZnS under excitation at 375 nm, the insets are excitation spectra. **b** The standard CIE coordinate color graph of ZnSe/ZnS/

ZnS QDs, insert shows the photographs of the ZnSe/ZnS/ZnS taken under daylight (left) and UV light (right)

QDs is improved after the ZnS shell is grown, especially the second ZnS shell increases the electron and hole wave functions overlap. On the other hand, the PL intensity is also improved by introducing the MPA as an effective stabilizer for the QDs, which is beneficial to inhibit auger recombination and reduce the energy transfer between the adjacent QDs [41]. In addition, as the shell thickness increases, an obvious red shift occurs in the PL spectra, which is attributed to the partial leakage of the electrons and holes, and also indicates that the ZnSe(S) alloy structure is not formed during the growth of the ZnS shell [32].

The standard CIE coordinate color graph of ZnSe/ZnS/ZnS QDs is shown in Fig. 5b. It is notable that the ZnSe/ZnS/ZnS QDs have good dispersion in water and remain the stability for at least 30 days without sedimentation. The insert of Fig. 5b shows a ZnSe/ZnS/ZnS solution synthesized over 30 days before the date of the photographs.

To obtain the ideal PL performance of ZnSe/ZnS/ZnS QDs, the synthesis conditions including the molar ratio of reactants, solution pH, reaction time, and temperature are optimized. The experimental results depicted in Fig. 6. Show that the QDs have the highest PL intensity at the following conditions:  $n(\text{Zn}^{2+}) : n(\text{Se}^{2-}) : n(\text{MPA}) = 1 : 0.5 : 1.2$ , the solution pH is 10.30, the reaction temperature and time are 100 °C and 4.5 h, respectively.

It is known that the QDs surface defects and non-radiative surface suspended bonds will quench the

PL of QDs and affect the stability of QDs. Therefore, we add  $\text{Zn}^{2+}$ , MPA, and thiourea in ZnSe QDs solution, and thiourea will slowly decompose into  $\text{S}^{2-}$  under alkaline conditions. Then  $\text{S}^{2-}$  react with  $\text{Zn}^{2+}$  to generate ZnS shell on ZnSe core. In this case, carriers are effectively confined in the ZnSe core, keeping them away from surface defects and hanging bonds, reducing PL quenching. Therefore, the thickness of the ZnS shell is crucial to the PL properties of ZnSe QDs.

In what follows, we investigate the influence of the thickness of the ZnS shell on the PL intensity of ZnSe QDs. Figure 7a shows the effects of the amount of ZnS precursor solutions on the PL intensity of QDs. The results show that the PL intensity is the highest when the molar ratio of ZnS precursor to ZnSe quantum dot solution is 1.5:1, and then the PL intensity decreases with the addition of ZnS precursor solution. The main reason is that a small amount of ZnS precursor cannot form an effective ZnS shell, but the excessive ZnS precursor solution, in addition to forming ZnS shell, the remaining  $\text{Zn}^{2+}$  will adhere to the surface of quantum dots, making quantum dots unstable, thereby reducing the PL intensity [42].

The effect of ZnS growth layers on the PL intensity is shown in Fig. 7b. One can see that the highest PL intensity appears when two layers of ZnS are growing on ZnSe (ZnSe/ZnS/ZnS). The main reason is that the single ZnS shell (ZnSe/ZnS) cannot provide a sufficient energy barrier to prevent the leakage of

**Fig. 6** Effects of molar ratio of reactants (a), solution pH (b), reaction temperature (c), and time (d) on the PL intensity of QDs,  $\lambda_{\text{ex}} = 375 \text{ nm}$

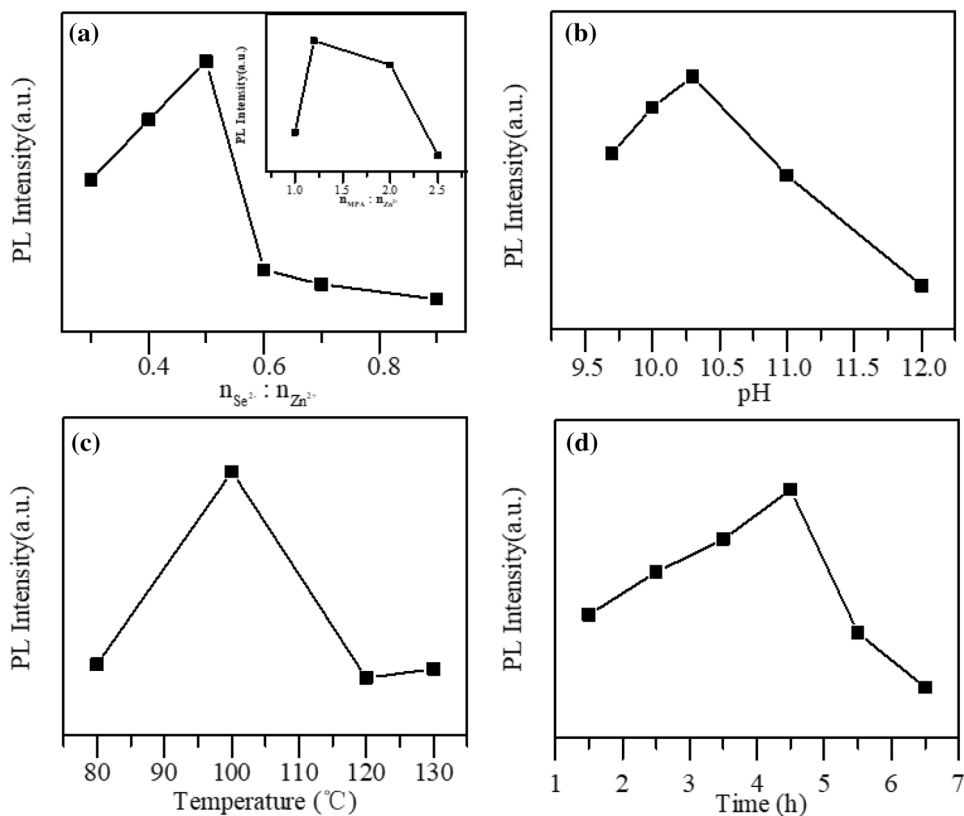
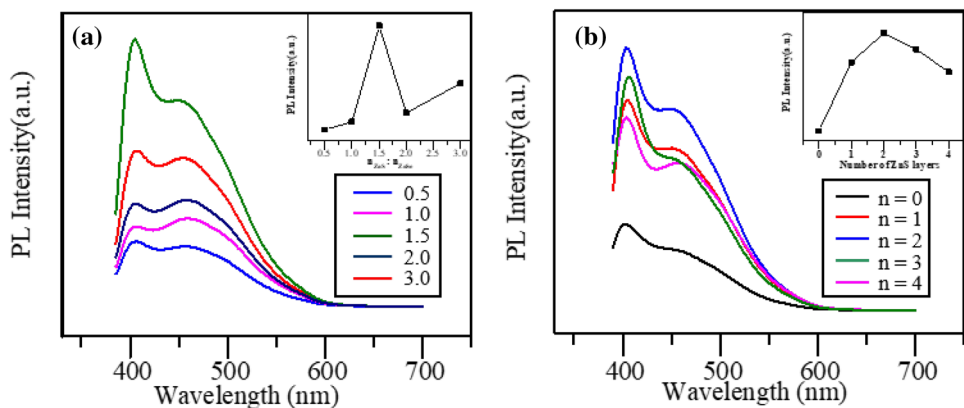


**Fig. 7** Effects of molar ratio of ZnS precursor solution to ZnSe QDs solution (a) and the number of ZnS layers (b) on the PL intensity of QDs,  $\lambda_{\text{ex}} = 375 \text{ nm}$



excitons, resulting in electrons and holes partially leaking to the ZnS shell [32]. Furthermore, the wave functions of electrons and holes are further limited due to the second ZnS shell, which can effectively handicap the luminescence quenching of QDs [33]. Nevertheless, the PL intensity of the prepared QDs decreases when the number of layers is greater than two, the reason is that the lattice mismatch between ZnSe and ZnS causes strain energy, and is eventually released in the form of islands or defects, which will reduce PL intensity [43]. In addition, there are still some  $\text{Zn}^{2+}$  vacancies on the surface of the ZnS shell,

and these vacancies are prone to non-radiative recombination, which also reduces the PL intensity of QDs.

## 4 Conclusion

In conclusion, we have developed a simple and efficient method for synthesizing water-soluble ZnSe/ZnS/ZnS QDs and studied the influence of preparation conditions on the PL intensity. It was concluded that the shell thickness of QDs was of significance in

the PL intensity of QDs. The ZnSe/ZnS/ZnS QDs with the highest PL intensity were obtained by successively growing the shell, and the PL intensity of ZnSe/ZnS/ZnS is 3.1 and 1.3 times as large as that of ZnSe and ZnSe/ZnS. In addition, the prepared QDs have good dispersion in water and remain the stability for at least 30 days without sedimentation. Our findings give a competitive candidate for developing the environment-friendly QDs in the applications of luminescence, display, especially in biological analysis.

## Acknowledgments

This work was supported by the National Natural Science Foundation of China (Grant No. 11674267, 51272215).

## Authors contribution

XL: methodology, experiment and writing original draft. HZ and BY: analysis and experiment. MW and WW: data processing and methodology. XZ: supervision and funding acquisition.

## Funding

The Funded was provided by National Natural Science Foundation of China, Grant Nos. (11674267, 51272215).

## Data availability

The data that support the findings of this study are open available in references.

## Declarations

**Conflict of interest** We declare that they have no known competing financial interests or personal relationships that could have appeared to influence the work reported in this paper.

**Ethical approval** We confirm that we comply with ethical standards.

## References

1. X. Dai, Z. Zhang, Y. Jin, Y. Niu, H. Cao, X. Liang, L. Chen, J. Wang, X. Peng, *Nature* **515**, 96–99 (2014)
2. H. Shen, Q. Gao, Y. Zhang, Y. Lin, Q. Lin, Z. Li, L. Chen, Z. Zeng, X. Li, Y. Jia, S. Wang, Z. Du, L.S. Li, Z. Zhang, *Nat. Photonics* **13**, 192–197 (2019)
3. Y.H. Won, O. Cho, T. Kim, D.Y. Chung, T. Kim, H. Chung, H. Jang, J. Lee, D. Kim, E. Jang, *Nature* **575**, 634–638 (2019)
4. T. Kim, K.H. Kim, S. Kim, S.M. Choi, H. Jang, H.K. Seo, H. Lee, D.Y. Chung, E. Jang, *Nature* **586**, 385–389 (2020)
5. P. Liu, Y. Lou, S. Ding, W. Zhang, Z. Wu, H. Yang, B. Xu, K. Wang, X.W. Sun, *Adv. Funct. Mater.* **31**, 2008453 (2021)
6. H. Li, J. Jiao, Q. Ye, Z. Wu, D. Luo, D. Xiong, *J. Mater. Sci. Mater. Electron.* **32**, 22024–22034 (2021)
7. Q. Xu, L. Meng, K. Sinha, F.I. Chowdhury, J. Hu, X. Wang, *ACS Photonics* **7**, 1297–1303 (2020)
8. L. Etgar, D. Yanover, R.K. Čapek, R. Vaxenburg, Z. Xue, B. Liu, M.K. Nazeeruddin, E. Lifshitz, M. Grätzel, *Adv. Funct. Mater.* **23**, 2736–2741 (2013)
9. R.M. Aoki, E.T.S. dos Torres, J.P.A. de Jesus, S.A. Lourenço, R.V. Fernandes, E. Laureto, M.A. Toledo da Silva, *J. Lumin.* **237**, 118178 (2021)
10. V. Kadam, C. Jagtap, T. Alshahrani, F. Khan, M.T. Khan, N. Ahmad, A. Al-Ahmed, H. Pathan, *J. Mater. Sci. Mater. Electron.* **32**, 28214–28222 (2021)
11. Y. Xu, Y. Lv, R. Wu, J. Li, H. Shen, H. Yang, H. Zhang, L.S. Li, *Inorg. Chem.* **60**, 6503–6513 (2021)
12. H. Yang, Q. Zhao, X. Wang, Y. Wu, Y. Su, W. Wei, *Sensors Actuators B Chem.* **337**, 129782 (2021)
13. H. Mattoussi, G. Palui, H. Bin Na, *Adv. Drug Deliv. Rev.* **64**, 138–166 (2012)
14. P. Rastogi, F. Palazon, M. Prato, F. Di Stasio, R. Krahné, *A.C.S. Appl. Mater. Interfaces.* **10**, 5665–5672 (2018)
15. J. Song, O. Wang, H. Shen, Q. Lin, Z. Li, L. Wang, X. Zhang, L.S. Li, *Adv. Funct. Mater.* **29**, 1808377 (2019)
16. X. Yang, Z.H. Zhang, T. Ding, N. Wang, G. Chen, C. Dang, H.V. Demir, X.W. Sun, *Nano Energy* **46**, 229–233 (2018)
17. F. Cao, Q. Wu, Y. Sui, S. Wang, Y. Dou, W. Hua, L. Kong, L. Wang, J. Zhang, T. Jiang, X. Yang, *Small* **17**, 2100030 (2021)
18. L.N. Kolonel, *Cancer* **37**, 1782–1787 (1976)
19. L. Järup, *Br. Med. Bull.* **68**, 167–182 (2003)
20. H. Shen, H. Wang, X. Li, J. Z. Niu, H. Wang, X. Chen, L. S. Li, *Dalt. Trans.* 10534–10540 (2009)
21. K. Senthilkumar, T. Kalaivani, S. Kanagesan, V. Balasubramanian, *J. Mater. Sci. Mater. Electron.* **23**, 2048–2052 (2012)
22. J. Zhang, J. Li, J. Zhang, R. Xie, W. Yang, *J. Phys. Chem. C* **114**, 11087–11091 (2010)
23. P. Reiss, M. Protière, L. Li, *Small* **5**, 154–168 (2009)

24. Y. Li, G. Han, H. Zou, L. Tang, X. Zhao, *Materials* **14**, 3066 (2021)
25. H. Chen, M. Wang, Y. Qi, Y. Li, X. Zhao, *Nanomaterials* **11**, 1061 (2021)
26. E. Molahossieni, M. Molaei, M. Karimipour, F. Amirian, *J. Mater. Sci. Mater. Electron.* **31**, 387–393 (2020)
27. X. Xue, L. Chen, C. Zhao, L. Chang, *J. Mater. Sci. Mater. Electron.* **29**, 9184–9192 (2018)
28. B. Goswami, S. Pal, P. Sarkar, *J. Phys. Chem. C* **112**, 11630–11636 (2008)
29. V.V. Nikesh, S. Mahamuni, *Semicond. Sci. Technol.* **16**, 687–690 (2001)
30. Z. Fang, Y. Li, H. Zhang, X. Zhong, L. Zhu, *J. Phys. Chem. C* **113**, 14145–14150 (2009)
31. A. Wang, H. Shen, S. Zang, Q. Lin, H. Wang, L. Qian, J. Niu, L.S. Li, *Nanoscale* **7**, 2951–2959 (2015)
32. B. Dong, L. Cao, G. Su, W. Liu, *Chem. Commun.* **46**, 7331–7333 (2010)
33. X. Bai, F. Purcell-Milton, Y.Kun'ko, *CrystEngComm* **23**, 6792–6799 (2021)
34. V. Wood, J.E. Halpert, M.J. Panzer, M.G. Bawendi, V. Bulović, *Nano Lett.* **9**, 2367–2371 (2009)
35. Z. Yang, Q. Wu, X. Zhou, F. Cao, X. Yang, J. Zhang, W. Li, *Nanoscale* **13**, 4562–4568 (2021)
36. C. Wang, X. Gao, Q. Ma, X. Su, *J. Mater. Chem.* **19**, 7016–7022 (2009)
37. C. Wang, S. Xu, Y. Wang, Z. Wang, Y. Cui, *J. Mater. Chem. C* **2**, 660–666 (2014)
38. L. Huang, H.-Y. Han, *Mater. Lett.* **64**, 1099–1101 (2010)
39. J. Kwon, S.W. Jun, S.I. Choi, X. Mao, J. Kim, E.K. Koh, Y.-H. Kim, S.K. Kim, D.Y. Hwang, C.S. Kim, J. Lee, *Sci. Adv.* **5**, 0044 (2021)
40. S.L. Zhang, C.F. Lin, Y.L. Weng, L.C. He, T.L. Guo, Y.A. Zhang, X.T. Zhou, *J. Mater. Sci. Mater. Electron.* **29**, 16805–16814 (2018)
41. J. Lim, B.G. Jeong, M. Park, J.K. Kim, J.M. Pietryga, Y.S. Park, V.I. Klimov, C. Lee, D.C. Lee, W.K. Bae, *Adv. Mater.* **26**, 8034–8040 (2014)
42. P. Wu, Z. Fang, X. Zhong, Y.J. Yang, *Colloids Surf. A Physicochem. Eng. Asp.* **375**, 109–116 (2011)
43. J. Cao, Z.J. Jiang, *J. Phys. Chem. C* **124**, 12049–12064 (2020)

**Publisher's Note** Springer Nature remains neutral with regard to jurisdictional claims in published maps and institutional affiliations.